Modelling interactions of acid-base balance and respiratory status in the toxicity of metal mixtures in the American oyster *Crassostrea virginica*

Brett M. Macey, Matthew J. Jenny, Heidi R. Williams, Lindy K. Thibodeaux, Marion Beal, Jonas S. Almeida, Charles Cunningham, Annalaura Mancia, Gregory W. Warr, Erin J. Burge, A. Fred Holland, Paul S. Gross, Sonomi Hikima, Karen G. Burnett, Louis Burnett, Robert W. Chapman

PII: S1095-6433(09)01180-5
DOI: doi: 10.1016/j.cbpa.2009.11.019
Reference: CBA 8865

To appear in: *Comparative Biochemistry and Physiology*

Received date: 22 June 2009
Revised date: 17 November 2009
Accepted date: 18 November 2009

Please cite this article as: Macey, Brett M., Jenny, Matthew J., Williams, Heidi R., Thibodeaux, Lindy K., Beal, Marion, Almeida, Jonas S., Cunningham, Charles, Mancia, Annalaura, Warr, Gregory W., Burge, Erin J., Holland, A. Fred, Gross, Paul S., Hikima, Sonomi, Burnett, Karen G., Burnett, Louis, Chapman, Robert W., Modelling interactions of acid-base balance and respiratory status in the toxicity of metal mixtures in the American oyster *Crassostrea virginica*, *Comparative Biochemistry and Physiology* (2009), doi: 10.1016/j.cbpa.2009.11.019

CBP ms.17266 Revised – part A

Modelling interactions of acid-base balance and respiratory status in the toxicity of metal mixtures in the American oyster *Crassostrea virginica*

Brett M. Macey[a,b,h], Matthew J. Jenny[g], Heidi R. Williams[a,b], Lindy K. Thibodeaux[a,b], Marion Beal[a,c], Jonas S. Almeida[d], Charles Cunningham [a,d,f], Annalaura Mancia[a,d], Gregory W. Warr[a,d,i], Erin J. Burge[a,b,e], A. Fred Holland[a], Paul S. Gross[a,d], Sonomi Hikima[a,d], Karen G. Burnett[a,b], Louis Burnett[a,b], Robert W. Chapman[a,b, c,d*]

[a]Hollings Marine Laboratory (HML), Charleston, SC 29412, USA; [b]Grice Marine Laboratory, College of Charleston, Charleston, SC 29412, USA; [c]Marine Resources Research Institute, South Carolina Department of Natural Resources, Charleston, SC 29412, USA; [d]Medical University of South Carolina, Charleston, SC 29425, USA

Current affiliations: [e]Department of Marine Science, Coastal Carolina University, Conway, SC 29526, USA; [f]Department of Biology, University of New Mexico, Albuquerque, NM 87131, USA; [g]Woods Hole Oceanographic Institution, Woods Hole, MA 02543, USA; [h]Department of Environmental Affairs and Tourism, Marine and Coastal Management, Roggebaai 8012, RSA, [i]Division of Molecular and Cellular Biosciences, National Science Foundation, Arlington VA 22230, USA.

*Corresponding author:
Hollings Marine Laboratory, 331 Fort Johnson Road, Charleston, South Carolina 29412, USA
phone: (843)762-8860; fax: (843)762-8737
e-mail: chapmanr@dnr.sc.gov

Abbreviations: ANN: artificial neural network; LPx: lipid peroxidation; TBARS: thiobarbituric acid-reactive substances; ROS: reactive oxygen species; THC: total hemocyte count; GSH: glutathione; TSA: tryptic soy agar; TCBS: thiosulfatecitrate-bile-sucrose; GLM: general linear models

Abstract

Heavy metals, such as copper, zinc and cadmium, represent some of the most common and serious pollutants in coastal estuaries. In the present study, we used a combination of linear and artificial neural network (ANN) modelling to detect and explore interactions among low-dose mixtures of these heavy metals and their impacts on fundamental physiological processes in tissues of the Eastern oyster, *Crassostrea virginica*. Animals were exposed to Cd (0.001 – 0.400 μM), Zn (0.001 – 3.059 μM) or Cu (0.002 – 0.787 μM), either alone or in combination for 1 to 27 days. We measured indicators of acid-base balance (hemolymph pH and total CO_2), gas exchange (Po_2), immunocompetence (total hemocyte counts, numbers of invasive bacteria), antioxidant status (glutathione, GSH), oxidative damage (lipid peroxidation; LPx), and metal accumulation in the gill and the hepatopancreas. Linear analysis showed that oxidative membrane damage from tissue accumulation of environmental metals was correlated with impaired acid-base balance in oysters. ANN analysis revealed interactions of metals with hemolymph acid-base chemistry in predicting oxidative damage that were not evident from linear analyses. These results highlight the usefulness of machine learning approaches, such as ANNs, for improving our ability to recognize and understand the effects of sub-acute exposure to contaminant mixtures.

Keywords: heavy metals, artificial neural networks, *Crassostrea virginica*, lipid peroxidation, glutathione, acid-base balance, hemolymph PO_2

1. Introduction

Industrialization and urbanization along the coastline of the US have substantially increased the amount and variety of anthropogenic pollutants entering estuarine ecosystems. Among the most common of these contaminants, heavy metals are of particular concern because they persist in the environment and have a wide variety of adverse effects. Developing biomarkers and predicting effects of contaminant mixtures, has garnered much attention in both human health and ecological risk assessments (Carpenter et al. 2002; Yang et al. 2007; Wang et al. 2008) with the general recognition that the relationship among these mixture components and their biological effects is both intricate and complex (Sexton et al. 2007). For heavy metal mixtures this complexity is driven in part by the fact that many of these metals interact with a wide but

common set of cellular targets, but may differ in affinity for these targets by many orders of magnitude (Viarengo 1989a).

We hypothesized that the relationship among heavy metals and their physiological effects might be detected and modelled using a combination of linear and artificial neural network (ANN) approaches. ANNs have been used to develop predictive models of other complex systems such climate change (Cannon et al. 2002, among others) and disease status in humans based upon gene expression profiles (Khan et al. 2001; Linder et al. 2004; Dankbar et al. 2007, among others).

To test this hypothesis, we characterized the physiological effects of environmentally-relevant low-dose mixtures of Cu, Cd, and Zn (Sanger et al. 1999), either alone or in combination for periods from 1 – 27 days, in the Eastern oyster, *Crassostrea virginica*. This ecologically and economically important bivalve mollusc lives in close association with estuarine sediments where its sessile nature and filter-feeding habit maximize the accumulation of contaminants in their tissues in concentrations high above those found in the surrounding seawater (Jenny et al. 2002).

In oysters, as in other organisms, Cu, Cd and Zn exist as divalent cations which are free or complexed to different classes of biological ligands. Cd is a trace metal with no known biological function, while Cu and Zn are essential elements and, as such, are required to maintain cellular homeostasis. In oysters, the gill and the hepatopancreas (digestive gland) are the primary tissues involved in the accumulation and detoxification of heavy metals, such as Cu, Zn and Cd (Marigómez et al. 2002; Sokolova et al. 2005). Heavy metals enhance the intracellular formation of toxic reactive oxygen species (ROS) (Stohs et al. 1995b; Ringwood et al. 1998; Geret et al. 2002b; Dailianis et al. 2005). Thus, metal-binding proteins and antioxidant enzymes, such as glutathione (GSH) and metallothioneins (MTs) are important detoxification elements that are induced to maintain the balance between pro- and antioxidative systems in cells (Dovzhenko et al. 2005). Indeed, studies have shown that surplus ROS can alter the structure of cell membranes by stimulating the peroxidation of membrane lipids. Thus, for the present study, oysters were exposed to Cd, Zn, or Cu, either alone or in combination, for periods from 1 – 27 days and indicators of antioxidant defense (GSH), oxidative damage (lipid peroxidation; LPx), immunocompetence (total hemocyte counts, numbers of invasive bacteria), as well as blood gas and acid-base balance (hemolymph PO_2, pH, total CO_2) were measured for each animal. The experimental design optimized input data for ANN analysis, which requires little or no

understanding of the mechanistic associations of the measured variables, but does require considerable volumes of data. This design contrasts with traditional statistical approaches which require extensive knowledge of the system, but comparatively little data. Perhaps more succinctly traditional linear analysis fits data to models, but ANN's extracts models from data. ANN's do not require independence among the input variables (independent variables in linear regression). Furthermore, in the application of machine learning approaches, the preference is for limited or no replication of the experimental conditions, so the ANNs learn rather than memorize. For these and other reasons they have been used extensively in medical, engineering, physics and atmospheric sciences (Almeida, 2002, Cannon et al. 2002 Khan et al. 2001; Linder et al. 2004; Dankbar et al. 2007, Chapman *et al.* 2009) . Detailed explanations of the approach can be found in Bishop (1996a,b Bishop 2006). Our approach was a compromise between the requirements of linear statistics and of machine learning provided by ANNs. First, correlations among the experimental variables were examined by linear statistical tools to provide statistical power. Subsequently, ANN analysis was employed to explore the higher dimensional interactions among metal mixtures on the oyster's physiological response.

2. Materials and Methods

2.1. Animal collection and maintenance

Adult Eastern oysters, *Crassostrea virginica* (Gmelin), from Taylor Shellfish Farms (Shelton, WA) were held for 30 days in well-aerated recirculating natural seawater systems at 25 ppt salinity and 20 – 22 ° C on a 12 h light cycle. During this period oysters were fed a mixed algal suspension (Shellfish Diet 1800®, Reed Mariculture) every second day.

2.2. Basic experimental protocol

One day prior to the start of the experiment, 4 oysters were placed in each of 54 five L beakers. Beakers contained four L of well-aerated filtered (0.45 µm) seawater maintained at 25 ppt salinity and 18 ± 1 °C. At the start of the 27 day experiment (Day 0), beakers were dosed with single or multiple metals at environmentally relevant doses (Table 1): Cd (0.001 – 0.400 µM), Zn (0.001 – 3.059 µM) or Cu (0.002 – 0.787 µM). Thereafter, the seawater in each beaker was routinely exchanged every second day, at which time metals were replenished in each beaker to their predetermined concentrations, and algal suspension added to facilitate metal uptake by the

oysters. Food was withheld from oysters at least 24 h before they were sampled. Sampling of oysters began on day 1 of the 27 day metal study, with 1 oyster sampled per day from each of 8 beakers. Sampling began with beaker number one and continued to beaker 54, then back to beaker one, continuing for 27 days until all 216 samples had been exhausted. The study design was not consistent with a typical dose-response model based on linear statistics; instead this design generated 216 individual treatments that ultimately could be analyzed by ANNs. A total of 8 animals were found dead or moribund at the time of sampling; these oysters were not associated with any particular dosing regimen and were excluded from the study. Each sampled oyster was blotted dry with a paper towel and weight, length, and width were recorded. Hemolymph (2 separate samples) was sampled anaerobically from the adductor muscle of each oyster using a 1 mL glass syringe fitted with a 23-ga needle. The dead space in the needle and syringe was filled with nitrogen-saturated distilled water to reduce contamination of the sample by atmospheric oxygen; the syringe was placed on ice prior to sampling. To gain access to the adductor muscle, the shell of the oyster was quickly notched along the posterior margin using pliers, exposing the muscle. Immediately following hemolymph withdrawal, oysters were placed on ice for dissection and tissue processing. Specific procedures are described below.

2.3. Quantification of total hemocyte count (THC) and culturable bacteria in hemolymph

Approximately 0.5 mL of hemolymph was withdrawn from the adductor muscle of each oyster. An aliquot of this sample was fixed with neutral buffered formaldehyde and hemocytes counted with a hemocytometer (Macey et al. 2008). For total counts of culturable bacteria, a second aliquot of the original hemolymph sample was overlayed in marine agar on TSA supplemented with 2.0% NaCl; for total culturable *Vibrio*, a second 100 µL aliquot of hemolymph was overlayed in marine again and cultured on TCBS agar supplemented with 1.5% NaCl (Macey et al. 2008). Data were expressed as total bacteria and *Vibrio* spp. mL^{-1} of hemolymph according to growth on TSA and TCBS plates, respectively.

2.4. Hemolymph variables

A second hemolymph sample was withdrawn from the adductor muscle of each oyster to assess hemolymph gas and acid-base chemistry. All instruments were thermostatted to 18 ± 0.1 °C. The partial pressure of oxygen (PO_2) in the hemolymph was determined with a Radiometer PHM

pH/blood gas monitor and PO_2 electrode. Hemolymph pH was determined with a Radiometer (BMS2 Mk2 Blood Micro System) capillary pH electrode and PHM pH/blood gas monitor that had been calibrated at experimental temperatures with precision Radiometer buffers. Total carbon dioxide, i.e., all forms of CO_2 including molecular CO_2, HCO_3^-, $CO_3^=$, and carbamino CO_2, in the hemolymph was determined with a Capni-Con 5 total CO_2 analyzer (Cameron Instrument Company).

2.5. Oyster dissection and tissue processing.

The right valve of each oyster was removed by breaking the hinge of the shell and removing the gills and the hepatopancreas to separate weigh boats. Tissues were minced and approximately 0.02 g (minimum) and 0.05 g (maximum) samples of the minced tissues were transferred to separate cryotubes, flash frozen in liquid nitrogen and stored at −80 °C until they were used for the GSH, LPx and metal content assays (see below).

2.6. Lipid peroxidation (LPx) and glutathione (GSH) assays.

Lipid peroxidation (LPx) in the gill and hepatopancreas of *C. virginica* was measured using a colorimetric assay that quantifies lipid degradation products based on the formation of total thiobarbituric acid reactive substances (TBARS) with malondialdehyde (TBARS) as the standard (Ringwood et al. 1999b). GSH concentrations of individual oyster tissues were determined using the glutathione reductase recycling assay described by Ringwood et al. (1999b).

2.7. Analysis of metal content

Tissues were digested in concentrated nitric acid at 160 °C at 210 psi and 225 watt for 6 min. Cooled samples were spiked with yttrium standard (10 ppm final concentration) and analyzed for Cu, Cd and Zn content by Inductively Coupled Plasma-Atomic Emission Spectroscopy. The National Bureau of Standards (NBS) Mussel Reference Material #1974b and Pygmy Sperm Whale Reference Material # QC03-LH3 were analysed with the samples to verify the metal analysis; the percent recoveries over all batches were 101.67 ± 11.74, 101.87 ± 11.14, and 99.00 ± 10.99% (mean ± S.D.) for Cu, Zn and Cd, respectively, for the Whale Reference Material and 106.78 ± 5.52, 95.74 ± 4.70, and 106.97 ± 9.21%, respectively, for the Mussel Reference Material.

2.8. Statistical analysis

To determine the effect of metal exposure on the tissue accumulation of each metal and to assess potential relationships between tissue metal content and physiological responses, data were analyzed initially by linear statistics using SigmaStat 3.1 and SYSTAT 11 software. Correlations between tissue content of each metal and physiological measures were investigated using Pearson's Product Moment Correlation procedure. All tests for normality (Kolmogorov-Smirnov test) or equal variances failed, therefore, correlation analyses were performed on rank transformed data. One-way ANOVA was used to test for differences in concentrations of each metal between the gills and the hepatopancreas of oysters exposed to metals and was also used to test for differences between basal concentrations of each metal in each tissue of oysters not exposed to metals. All tests for normality or equal variances failed, therefore, a Kruskal-Wallis ANOVA on Ranks test was used to test for significant differences. Interactions between metal content of each tissue and physiological responses were assessed by analysis of variance (ANOVA) using General Linear Models (GLM) in SYSTAT 11. Since all test for normality and equal variance failed, GLM on quantile-normalized data were used to test for significant interactions. Each GLM consisted of 3 independent variables [tissue (gill or hepatopancreas) Cu, Zn and Cd] and one dependent variable [tissue (gill or hepatopancreas) TBARS]. Significance was assigned at $p \leq 0.05$ for all analyses. Subsequently, ANNs were used to model potential interactions of tissue metal contents and hemolymph measures in predicting tissue oxidative damage (LPx) or antioxidant status (GSH). Each of the ANNs consisted of 6 input variables [hemolymph pH, total CO_2, PO_2, and tissue (gill or hepatopancreas) Cu, Zn and Cd] with one output variable. For each output variable (gill LPx, gill GSH, hepatopancreas LPx and hepatopancreas GSH), separate ANNs (n = 30) were developed using WebNeuralNet 1.0 (Almeida 2002). All variables were scaled to their non-parametric cumulative distributions by replacing the raw values with their rank/n (n = total data points) to overcome scale differences. The transformed data were then divided into two sets by random allocation; one comprising 90% of the records to train the ANN, while the remaining data were used as a cross validation (CV) set. A new subset of data was randomly selected before training each ANN to avoid bias in the selection of the CV set. Each ANN was first trained using both the input and output data of the training set, which consisted of 187 data points from each of the input and output variables. To prevent over training the ANNs, an early stopping procedure (Almeida 2002) was employed. After each ANN was trained, the withheld data points from the CV set were analyzed to evaluate

the predictive capabilities of the ANN. In essence, this was achieved by calculating the R-squared (R^2) values for the outputs of each ANN and the observed values of the accompanying CV sets, and comparing the CV set predictions with those generated by the appropriate ANN. Next, the impact of each input variable (hemolymph pH, total CO_2, PO_2, tissue Cu, Cd, Zn) was examined by computing the sensitivities of the outputs to changes in the inputs (Heshem, 1992) for all ANNs in which the model and CV set R^2 value were greater than the median value for all 30 ANNs. The interactions of the inputs on the outputs were examined using a derivative of the approach of Cannon and McKendry (2002), where the two variables with the highest sensitivities were allowed to vary in 5% increments over the scaled range and all other input variables were held to their mean (50%) values. These 'artificial' data were then fed to the ANN models with the largest R^2 values to predict the output value and the results plotted on three-dimensional surfaces.

3. Results

3.1. Metal accumulation in the tissues of C. virginica.

Overall, measured concentrations of Cu, Cd and Zn ($\mu g\ g^{-1}$ wet weight tissue) were higher in the hepatopancreas than in the gills of oysters exposed to metals (one-way ANOVA; $P < 0.001$, < 0.001, $= 0.003$ and for Cu, Cd and Zn, respectively). Furthermore, basal concentrations of Cu and Zn were noticeably higher and more variable in the gills and the hepatopancreas when compared to basal Cd concentrations ($P < 0.001$). Tissue levels of the essential metals Cu and Zn were independent of the ambient water concentrations of the metals over the entire range of exposures (Fig. 1A, B). In contrast, cadmium, a non-essential metal, was the only metal that accumulated linearly with time in the gill ($r = 0.828$; $P < 0.001$) and the hepatopancreas ($r = 0.793$; $P < 0.001$) over the full range of Cd exposure concentrations (Fig. 1C). Cu contents were directly related to those of Zn in the gill ($n = 208$, $r = 0.0713$, $P < 0.001$) and in the hepatopancreas ($n = 208$, $r = 0.649$, $P < 0.001$). To a lesser degree, Cu content positively correlated with Cd content in the gill ($r = 0.216$, $P = 0.0018$), but not in the hepatopancreas. No other significant correlations were observed between measured metals in either tissue.

3.2. Correlation of measured tissue metals with physiological traits of C. virginica.

Since each of the 216 test animals represented a unique set of metal exposure parameters

(combination of metals, dose levels and duration), the resulting values could not be represented by standard descriptive statistics. Physiological data obtained from the 208 animals that survived the exposure period and yielded tissue samples (Figure 2) generally fell within ranges reported for *C. virginica* in control or low level metal exposures (Viarengo et al. 1990; Roméo et al. 1997; Ringwood et al. 1998; Ringwood et al. 1999a). Correlations between metal exposures and physiological measures were investigated using Pearson's Product Moment Correlation procedure. Exposure to Zn was negatively correlated with TBARS, indicators of oxidative membrane damage in the hepatopancreas, ($r = -0.150$, $P = 0.0304$), but not in the gill. No other significant relationships were noted between metal exposures and physiological measurements in oysters (data not shown). In contrast, tissue concentrations of individual metals were associated with several physiological measurements (Fig. 3A, B), most notably TBARS. In the gill, Cu ($r = 0.527$, $P < 0.001$), Cd ($r = 0.204$, $P = 0.0032$) and Zn ($r = 0.256$, $P < 0.001$) correlated positively with TBARS, as did Cu ($r = 0.618$, $P < 0.001$) and Zn ($r = 0.247$, $P < 0.001$) in the hepatopancreas. By comparison, metal associations with GSH were mixed. In the gill only Cu ($r = 0.203$, $P = 0.0033$) but not Zn or Cd positively correlated with antioxidant GSH, while both Cd ($r = -0.149$, $P < 0.001$) and Zn ($r = -0.95$, $P = 0.0049$) in the hepatopancreas were negatively associated with GSH in that tissue.

Several other significant correlations were noted (Fig. 3A, B). Gill Cd was associated with increased hemolymph pH ($r = 0.159$, $p = 0.0221$) while hepatopancreas Cu correlated with increased hemolymph pH (and $r = 0.284$, $P < 0.001$, respectively) and decreased total CO_2 ($r = -0.137$, $P = 0.0477$). Of the three metals, only Cu was associated with markers of immune function. Gill Cu was positively correlated with total culturable bacteria in the hemolymph ($r = 0.138$, $P = 0.0461$), while hepatopancreas Cu was negatively associated with THC ($r = -0.180$, $P = 0.0092$).

In the hepatopancreas there was a significant interaction between measured Cu and Zn when predicting oxidative damage, measured as TBARS (Table 2, GLM, $P = 0.014$), but not in the gill tissue. No additional significant interactions between the content of metals measured in gill and hepatopancreas were evident when predicting other physiological measurements of oysters, such as GSH, THC, hemolymph pH or total CO_2.

3.3. Artificial neural network analysis (ANN).

Because interactions among the metals were detected by linear analysis, ANNs were used to

explore these interactions in predicting LPx (measured as TBARS) and compared to models predicting GSH in the hepatopancreas and gill. The three respiratory measurements hemolymph pH, total CO_2 and PO_2 were included as input variables because the two acid-base components (pH, total CO_2) responded to tissue contents of all three metals. ANN models could more reasonably predict hepatopancreas than gill TBARS based on the metal content of the respective tissues. The mean R^2 value for hepatopancreas TBARS over all the ANN models was 0.50 ± 0.11 (Mean ± SD, n = 30), with some of the values approaching 0.7 (Table 3). By comparison, the mean R^2 value for gill TBARS over all models was 0.35 ± 0.11 (Table 4). Similarly, the cross-validation R^2 values for models predicting TBARS were 0.53 ± 0.14 (Table 3) and 0.24 ± 0.16 (Table 4) for the hepatopancreas and the gills, respectively, confirming the relative validity of the predictions made by each model. Furthermore, hepatopancreas TBARS appeared to be more consistently predictable than gill TBARS, as the variation in R^2 and cross-validation R^2 values with respect to the mean in each model were smaller for the hepatopancreas than for the gills (Tables 3, 4).

In contrast, GSH in both the gills and the hepatopancreas was poorly predicted by the input variables used for ANN modelling. The mean R^2 values for predicting GSH were only 0.07 ± 0.06 (Table 3) and 0.14 ± 0.11 (Table 4) for the gills and the hepatopancreas, respectively. Likewise, the mean cross-validation R^2 values and their variances for models predicting GSH in both tissue types were very low (Tables 3, 4).

A sensitivity analysis was conducted for the top performing ANNs to determine the contribution of each of the 6 input variables [hemolymph pH, total CO_2, PO_2, and tissue (gill or hepatopancreas) Cu, Cd or Zn] to the overall variance observed in each model predicting tissue TBARS. As GSH was poorly predicted by all ANN models in the present study, a sensitivity analysis was not conducted for these models. The best performing ANNs had model and cross-validation R^2 values greater than the median value for all 30 ANNs. Models 6 and 7 were chosen from the ANNs predicting hepatopancreas TBARS (Table 3), while Model 8 was chosen from ANNs predicting gill TBARS (Table 4). Sensitivity analysis reveals that in the hepatopancreas, the partial pressure of oxygen (PO_2) in the hemolymph is a dominant variable in both models (Fig. 4). Model 6 has the larger mean R^2 value. Model 7 has the larger cross-validation R^2 value and a smaller number of nodes (Table 4) and in most cases we would choose Model 7 over 6 for these reasons. However, as Model 6 indicates that Cu is more important than Zn in predicting TBARS (indicating LPx) and as this model confirms findings from the linear statistical analysis,

we would suggest that this is the preferred ANN model. Model 6 suggests that LPx in the hepatopancreas is more sensitive to changes in tissue Cu and Cd, and to hemolymph PO_2, than to any of the other measured variables (Fig. 4).

Sensitivity analysis indicated that each of the input variables contributed to the overall variance observed in Model 8 in predicting gill TBARS (Fig. 5). In the gill, as in the hepatopancreas, it is clear that the degree of oxidative membrane damage is more sensitive to changes in tissue Cu than to other input variables, but hemolymph pH, total CO_2 and PO_2 also make strong contributions to predicting TBARS. Moreover, summed Cu, Zn and Cd concentrations in both tissues appear to make significant contributions towards the overall variance observed in each model, emphasizing the cumulative detrimental effects of these metals on membrane integrity. The interactions of the more sensitive input variables (tissue Cu, hemolymph pH and hemolymph PO_2) in predicting TBARS in the gills and the hepatopancreas were graphically illustrated (Fig. 6A, B) using a modified form of the sensitivity analysis described by Cannon and McKendry (2002). Oxidative damage in the gill (TBARS) increased as hemolymph pH and tissue Cu concentrations increased and the effects are non-linear, but not strongly so (Fig. 6A). Similarly, hepatopancreas TBARS increased with increasing PO_2 in the hemolymph and with hepatopancreas Cu (Fig. 6B). These graphical surfaces clearly suggest complex, non-linear interactions between tissue Cu content and hemolymph pH or PO_2 in predicting tissue TBARS. Furthermore, the overall TBARS response is consistent with an increasingly oxidative environment.

4. Discussion

ANN models generated in the present study demonstrated that the responses of key toxicological indicators can be modelled and predicted from an appropriate set of input variables. While linear analyses provided correlative values of some individual metals to changes in hemolymph gasses and pH, ANN analysis suggested that the level of damage to cellular membranes was sensitive to tissue content of all three metals and strongly depended on other physiological measures, such as changes in hemolymph pH and PO_2 (Fig. 6). To our knowledge, this is the first study to show important metal-metal interactions as well as interactions of metal content with hemolymph gas and acid-base chemistry in predicting membrane damage in molluscs. It is particularly noteworthy that where low tissue Cu is accompanied by low pH or low PO_2 both hepatopancreas

and gill manifest the lowest predicted level of TBARS, while in those tissues with high Cu content along with high pH or high PO_2, the reverse is observed (Fig. 6). This is in keeping with our understanding of the response of TBARS to redox conditions, and the overall topography of the predicted response clearly suggests a non-linear interaction between metal content, hemolymph acid-base variables and TBARS. The contributions of hemolymph variables to the predictive power of the ANN models as observed in the present study could be explained by changes in ventilation rate of oysters as function of metal exposure or tissue burden, as reported for tropical oysters *Crassostrea belcheri* exposed to Cu (Elfwing et al. 2002). Alternatively, tissue metal burdens may be limited by ventilatory activity in bivalves as reported for Cd uptake in the Asiatic clam, *Corbicula fluminea* (Massabuau et al. 2003). Certainly, the resulting changes in gas exchange and acid-base physiology of oysters could influence a variety of biochemical processes, including the deposition of shell that is essential to oyster growth (Booth et al. 1984; Burnett 1988).

While linear regression techniques can generate response-surface plots, they cannot interrogate non-linear dynamics similar to those in Fig 6 without human intervention specifying the structure of the relationships. The advantage of the ANN's is that the mathematical architecture is infinitely flexible and does not require human intervention (e.g. bias). The various models produced by the analysis are not viewed as solutions, but rather as hypotheses of relationships amenable to further empirical tests.

In the present study, Cu, Zn and Cd tissue contents correlated with significant changes in LPx, as measured by elevated tissue levels of total TBARS. The influence of transition metals such as Cu on oxidative processes, resulting in the production of oxyradicals, has been described, and it is suggested that cupric ions are involved in both the initiation and propagation steps of LPx (reviewed by Viarengo 1989a). In fact, increases in LPx following exposure to Cu have been documented in the hard clam *Ruditapes decussatus* (Roméo et al. 1997), the Eastern oyster *Crassostrea virginica* (Ringwood et al. 1998), and the mussels *Mytilus galloprovincialis* (Viarengo et al. 1990) and *Mytilus edulis* (Geret et al. 2002a). While excess Cu can mediate free radical production directly via redox cycling, oxyradicals may also be formed indirectly via cupric ions binding to and adversely affecting metal-requiring antioxidants, such as GSH and MT (Ringwood et al. 1999a; Valko et al. 2005). In fact, it has been strongly suggested that there are multiple processes that bind copper and reduce its cellular toxicity (Valko et al. 2005). Conversely, non-redox metals, such as Cd, are unable to generate free radicals directly and

indirectly cause free radical-induced damage to important cellular macromolecules, particularly various complexes of the electron transport chain in mitochondria, and inhibit important cellular antioxidant enzymes and proteins, which may, in turn, stimulate LPx through oxidation of polyunsaturated fatty acids (Stohs et al. 1995a; Stohs et al. 2000; Dorta et al. 2003; Wang et al. 2004). The inverse association of Zn and Cd with GSH in the hepatopancreas observed in our study supports the idea that GSH provides early protection against oxidative stress from exposure to these metals, by binding of these metals to GSH or inhibition of GHS synthesis by these metals, until MTs can be induced (Quig 1998; Ringwood et al. 1998). That this effect was not noted for Cu in this study supports the notion that Cu ions, which can undergo redox cycling, are involved in both the initiation and propagation steps of LPx via the direct formation of reactive oxygen species, whereas Cd and Zn ions, which do not undergo redox cycling, stimulate LPx indirectly by binding to and inhibiting cellular antioxidants, such as GSH (Viarengo 1989a). This does not however exclude the possibility of the formation of Cu-GSH complexes, particularly since –SH groups of most metabolites and enzymes, including GSH, have a higher affinity for Cu than Cd or Zn (Viarengo 1989b). In fact, the discovery that the upper limit of "free" pools of Cu are far less than a single ion per cell strongly suggests that there is significant overcapacity for chelation of Cu in the cell and that multiple cellular antioxidants exist that bind Cu (Valko et al. 2005). However, Ringwood et al. (1998) suggested that conditions that cause depletion of important cellular antioxidants, such as GSH and MT, may enhance pollutant toxicity, suggesting that the impacts of exposure to metal mixtures are complex and potentially compounding. Indeed, the significant correlation between tissue contents of Cd and LPx as well as the general linear model identification of Zn-Cu interactions in predicting LPx of oysters in the present study supports this notion.

Cd suppresses the activity of many antioxidant enzymes and can displace Cu and Fe from cytoplasmic and membrane proteins which may then participate in ROS-producing Fenton reactions (Flipič et al. 2006). More specifically, Engel (1999) demonstrated that Cu can displace Cd from MT when oysters are exposed to these trace metals in combination, but that Cd is not lost from the tissues of the oyster. Furthermore, it is postulated that MT gene expression in oysters is regulated via a Zn-sensitive inhibitor, as is the case for regulation of MT gene expression in mice (Roesijadi 1996). Although MT induction via the displacement of Zn has yet to be empirically demonstrated in oysters, it is possible that this sort of metal-metal exchange reaction is responsible for the Zn-Cu interactions observed in oysters in the present study when

predicting tissue LPx.

The approach of combining general linear models and ANN analysis has revealed important metal-metal interactions as well as interactions of metal content with hemolymph gas and acid-base chemistry (hemolymph PO_2 as well as pH and total CO_2) in predicting peroxidation of membrane lipids that were not evident from linear analyses. These results support a growing body of evidence implicating the role of heavy metals in the peroxidation of membrane lipids and the disruption of important cellular antioxidants that play key roles in protecting cells against oxidative damage. This study also highlights the usefulness of machine learning approaches, such as ANNs, for improving our ability to recognize and understand the effects of sub-acute exposure to environmentally relevant concentrations of mixed contaminants.

5. Acknowledgements

This study was supported by NOAA's Center of Excellence in Oceans and Human Health at HML and the National Science Foundation. Any opinion, finding, conclusions or recommendations expressed in this material are those of the authors and do not necessarily reflect the views of the NSF. GML Contribution No. 348; MRD SCDNR Contribution ###.

References:

Almeida, J.S., 2002. Predictive non-linear modeling of complex data by artificial neural networks. Curr. Opin. Biotechnol. 13, 72-76.

Booth, C.E., McDonald, D.G., Walsh, P.J., 1984. Acid-base balance in the sea mussel, *Mytilus edulis*. I. Effects of hypoxia and air-exposure on hemolymph acid-base status. Mar. Biol. Lett. 5, 347-358.

Burnett, L.E., 1988. Physiological responses to air exposure: Acid-base balance and the role of branchial water stores. Am. Zool. 28, 125-135.

Cannon, A.J., McKendry, I.G., 2002. A graphical sensitivity analysis for statistical climate models: application to Indian monsoon rainfall prediction by artificial neural networks and multiple linear regression models. Int. J. Climatol. 22, 1687-1708.

Carpenter, D.O., Arcaro, K., Spink, D.C., 2002. Understanding the human health effects of chemical mixtures. Environ. Health Perspect. 110, 25-42.

Dailianis, S., Piperakis, S.M., Kaloyianni, M., 2005. Cadmium effects on ROS production and DNA damage via adrenergic receptors stimulation: role of Na+/H+ exchanger and PKC. Free Radical Res 39, 1059-1070.

Dankbar, D.M., Dawson, E.D., Mehlmann, M., Moore, C.L., Smagala, J.A., Shaw, M.W., Cox, N.J., Kuchta, R.D., Rowlen, K.L., 2007. Diagnostic microarray for influenza B viruses. Anal. Chem. 79, 2084-2090.

Dorta, D.J., Leite, S., DeMarco, K.C., Prado, I.M.R., Rodrigues, T., Mingatto, F.E., Uyemura, S.A., Santos, A.C., Curti, C., 2003. A proposed sequence of events for cadmium-induced mitochondrial impairment. Journal of Inorganic Biochemistry 97, 251-257.

Dovzhenko, N.V., Kurilenko, A.V., Bel'cheva, N.N., Chelomin, V.P., 2005. Cadmium-induced oxidative stress in the bivalve mollusk *Modiolus modiolus*. Russ. J. Mar. Biol. 31, 309-313.

Elfwing, T., Tedengren, M., 2002. Effects of copper on the metabolism of three species of tropical oysters, *Saccostrea cucullata*, *Crassostrea lugubris* and *C. belcheri*. Aquaculture 204, 1157-1166.

Engel, D.W., 1999. Accumulation and cytosolic partitioning of metals in the American oyster *Crassostrea virginica*. Mar. Environ. Res. 47, 89-102.

Flipič, M., Fatur, T., Vudrag, M., 2006. Molecular mechanisms of cadmium induced mutagenicity. Hum. Exp. Toxicol. 25, 67-77.

Geret, F., Jouan, A., Turpin, V., Bebianno, M.J., Cosson, R.P., 2002a. Influence of metal exposure on metallothionein synthesis and lipid peroxidation in two bivalve mollusks: the oyster (*Crassostrea gigas*) and the mussel (*Mytilus edulis*). Aquat. Living Resour. 15, 61-66.

Geret, F., Serafim, A., Barreira, L., Bebianno, M.J., 2002b. Effect of cadmium on antioxidant enzyme activities and lipid peroxidation in the gills of the clam *Ruditapes decussatus*. Biomarkers 7, 242 - 256.

Jenny, M.J., Ringwood, A.H., Lacy, E.R., Lewitus, A.J., Kempton, J.W., Gross, P.S., Warr, G.W., Chapman, R.W., 2002. Potential Indicators of stress response identified by expressed sequence tag analysis of hemocytes and embryos from the American oyster, *Crassostrea virginica*. Mar. Biotechnol. 4, 81-93.

Khan, J., Ringér, M., Saal, L.H., Ladanyi, M., Wesermann, F., Berthold, F., Schwab, M., Antonescu, C.R., Peterson, C., Meltzer, P.S., 2001. Classification and diagnostic prediction of cancers using gene expression profiling and artificial neural networks. Nat. Med. 7, 673-679.

Linder, R., Dew, D., Sudhoff, H., Theegarten, D., Remberger, K., Poppl, S.J., Wagner, M., 2004. The 'subsequent artificial neural network' (SANN) approach might bring more classificatory power to ANN-based DNA microarray analyses. Bioinformatics 20:3544-3552.

Macey, B.M., Achilihu, I.O., Burnett, K., Burnett, L., 2008. Effects of hypercapnic hypoxia on inactivation and elimination of *Vibrio campbellii* in the Eastern oyster, *Crassostrea virginica*. Appl. Environ. Microbiol. 74, 6077-6084.

Marigómez, I., Soto, M., Cajaraville, M., Angulo, E., Giamberini, L., 2002. Cellular and subcellular distribution of metals in molluscs. Microsc. Res. Tech. 56, 358-392.

Massabuau, J.-C., Tran, D., 2003. Ventilation, a recently described step limiting heavy metal contamination in aquatic animals. J Physique. IV 107, 839-843.

Quig, D., 1998. Cysteine metabolism and metal toxicity. Altern. Med. Rev. 3, 262-270.

Ringwood, A.H., Conners, D.E., Dinovo, A., 1998. The effects of copper exposures on cellular responses in oysters. Mar. Environ. Res. 46, 591-595.

Ringwood, A.H., Conners, D.E., Keppler, C.J., Dinovo, A.A., 1999. Biomarker studies with juvenile oysters (*Crassostrea virginica*) deployed in-situ. Biomarkers 4, 400-414.

Roesijadi, G., 1996. Metallothionein and its role in toxic metal regulation. Comp. Biochem. Physiol. C 113, 117-123.

Roméo, M., Gnassia-Barelli, M., 1997. Effect of heavy metals on lipid peroxidation in the Mediterranean clam *Ruditapes decussatus*. Comp. Biochem. Physiol. C 118, 33-37.

Sanger, D.M., Holland, A.F., Scott, G.I., 1999. Tidal creek and salt marsh sediments in South Carolina coastal estuaries: I. Distribution of trace metals. Arch. Environ. Contam. Toxicol. 37, 445-457.

Sexton, K., Hattis, D., 2007. Assessing cumulative health risks from exposure to environmental mixtures - three fundamental questions. Environ. Health Perspect. 115, 825-832.

Sokolova, I.M., Ringwood, A.H., Johnson, C., 2005. Tissue-specific accumulation of cadmium in subcellular compartments of eastern oysters *Crassostrea virginica* Gmelin (Bivalvia: Ostreidae). Aquat. Toxicol. 74, 218-228.

Stohs, S.J., Bagchi, D., 1995. Oxidative mechanisms in the toxicity of metal ions. Free Radic. Biol. Med. 18, 321-336.

Stohs, S.J., Bagchi, D., Hassoun, E., Bagchi, M., 2000. Oxidative mechanisms in the toxicity of chromium and cadmium ions. J. Environ. Pathol. Toxicol. Oncol. 19, 201-213.

Valko, M., Morris, H., Cronin, M.T.D., 2005. Metals, toxicity and oxidative stress. Curr Med Chem 12, 1161-1208.

Viarengo, A., 1989. Heavy metals in marine invertebrates: mechanisms of regulation and toxicity at the cellular level. Rev. Aquat. Sci. 1, 295-317.

Viarengo, A., Canesi, L., Pertica, M., Poli, G., Moore, M.N., Orunesu, M., 1990. Heavy metal effects on lipid peroxidation in the tissues of *Mytilus galloprovincialis* LAM. Comp. Biochem. Physiol. C 97, 37-42.

Wang, G., Fowler, B.A., 2008. Roles of biomarkers in evaluating interactions among mixtures of lead, cadmium and arsenic. Toxicol. Appl. Pharmacol. 233, 92-99.

Wang, Y., Fang, J., Leonard, S.S., Krishna Rao, K.M., 2004. Cadmium inhibits the electron transfer chain and induces reactive oxygen species. Free Radical Biol Med 36, 1434-1443.

Yang, R.S.H., Dennison, J.E., 2007. Initial analyses of the relationship between "thresholds" of toxicity for individual chemicals and "interaction thresholds" for chemical mixtures. Toxicol. Appl. Pharmacol. 223, 133-138.

Figure Legends

Figure 1. (A) The tissue concentrations of Cu measured in the gill and the hepatopancreas of *Crassostrea virginica* held in Cu alone or in combination with other metals for 1 – 27 days. Total waterborne exposure to Cu (x-axis) is expressed as water concentration of Cu (μM) *days of exposure. Concentrations of Zn (B) and Cd (C) in the same tissues are displayed as a function of total waterborne exposure to Zn and Cd, respectively.

Figure 2. Box-and-whiskers plots of data from all experimental animals (n = 208) for each major physiological variable measured in this study. (A) TBARS and GSH values for the gill and the hepatopancreas (Hepato), (B) total hemocyte count (THC), (C) hemolymph P_{O_2} and total CO_2, (D) hemolymph pH, and (E) colony-forming units (CFU) mL^{-1} hemolymph on TSA or

TCBS agar. Box boundaries indicate 25th and 75th percentile, the line within the box marks the median value, and whiskers indicate the 10th and 90th percentiles. All values, including outliers are depicted.

Figure 3. Correlation coefficients (r-values) for significant associations between physiological measurements and measured metals in (A) the gill and (B) the hepatopancreas of *Crassostrea virginica* following exposure to each metal alone and in combinations for a period of 1 – 27 days. Analysis was performed using the Pearson Product Moment Correlation procedure on rank transformed data and significance was assigned at $P<0.05$. Non-significant interactions are not shown.

Figure 4. Sensitivities of TBARS in hepatopancreas to the input variables (metal contents, hemolymph pH, P_{O_2} and total CO_2) for the best performing models 6 and 7 from the ANN analysis.

Figure 5. Sensitivities of TBARS in the gill to the input variables (metal contents, hemolymph pH, P_{O_2} and total CO_2) for the best performing model 8 from the ANN analysis.

Figure 6. Theoretical projections of the response of TBARS to changes in the exposure levels of the indicated variable on the x and y axes. All variables have been scaled to their non-parametric values where 0 indicates the minimum and 1 indicates the maximum values observed in the data. (see text).

Table 1. Concentrations (µM) of $CuCl_2$, $ZnCl_2$ and $CdCl_2$ added to each beaker during the 27 day oyster metal challenge experiment.

Beaker #	Zinc	Copper	Cadmium
1	0.049	0.000	0.214
2	0.196	0.315	0.000
3	0.306	0.002	0.037
4	1.101	0.066	0.044
5	3.059	0.044	0.010
6	0.000	0.000	0.000
7	2.447	0.050	0.000
8	0.000	0.197	0.013
9	0.092	0.000	0.062
10	0.000	0.000	0.025
11	0.306	0.079	0.000
12	1.835	0.598	0.267
13	1.590	0.787	0.002
14	0.000	0.039	0.004
15	1.223	0.017	0.231
16	2.080	0.000	0.004
17	0.000	0.010	0.006
18	0.000	0.000	0.000
19	0.765	0.000	0.111
20	0.000	0.220	0.400
21	0.040	0.000	0.044
22	0.000	0.000	0.000
23	0.000	0.000	0.302
24	0.979	0.409	0.000
25	0.031	0.008	0.004
26	0.171	0.504	0.178
27	0.428	0.000	0.000
28	0.000	0.252	0.445
29	0.015	0.004	0.125
30	0.012	0.000	0.000
31	0.000	0.000	0.160
32	0.110	0.028	0.016
33	1.468	0.110	0.001
34	2.325	0.007	0.000
35	0.006	0.472	0.320
36	2.753	0.000	0.000
37	0.000	0.003	0.000
38	0.000	0.013	0.338
39	0.000	0.001	0.000
40	2.202	0.000	0.028
41	0.000	0.157	0.007
42	0.000	0.024	0.356

43	0.003	0.000	0.000
44	0.028	0.283	0.000
45	0.067	0.567	0.007
46	0.000	0.708	0.000
47	0.153	0.006	0.000
48	0.612	0.000	0.089
49	0.000	0.079	0.000
50	1.957	0.629	0.285
51	0.049	0.013	0.142
52	0.257	0.535	0.002
53	0.856	0.378	0.000
54	0.024	0.000	0.022

Table 2. Assessment of interactions between metal contents of hepatopancreas when predicting oxidation damage, measured as TBARS (General Linear Models). * significant interactions (P<0.05).

Effect	Coefficient	STD Error	STD Coefficient	Tolerance	t	P(2 Tail)
Constant	2.894	10.174	0.000	.0.284	0.777	
Cu	1.309	0.416	1.309	0.045	3.149	0.003*
Zn	0.777	0.399	0.777	0.049	1.949	0.056
Cd	-0.043	0.276	-0.043	0.102	-0.156	0.877
Cu*Zn	-0.026	0.010	-1.668	0.018	-2.525	0.014*
Cu*Cd	-0.004	0.011	-0.207	0.024	-0.360	0.720
Zn*Cd	-0.015	0.011	-0.809	0.022	-1.346	0.183
Cu*Zn*Cd	0.00	0.000	1.251	0.011	1.515	0.135

Table 3. ANN (n = 30) analysis of TBARS and GSH levels in the hepatopancreas of oysters exposed to Cu, Zn and/or Cd.

	Lipid Peroxidation (TBARS)			Glutathione (GSH)		
Model	**# Nodes**	**Model R2**	**CV R2**	**#Nodes**	**Model R2**	**CV R2**
1	9	0.4289	0.2652	9	0.1349	0.0866
2	9	0.3715	0.7326	7	0.1441	0.1110
3	5	0.6957	0.3642	5	0.3667	0.1649
4	7	0.5006	0.4938	5	0.0864	0.0328
5	7	0.3917	0.6919	5	0.0720	0.2296
6	7	0.6465	0.4681	7	0.1176	0.1654
7	5	0.6072	0.7002	7	0.3028	0.0688
8	5	0.3979	0.6905	9	0.1172	0.3552
9	7	0.5649	0.7380	6	0.3948	0.0058
10	5	0.6035	0.6459	7	0.0586	0.1656
11	6	0.6075	0.5286	5	0.1056	0.2849
12	5	0.6124	0.6212	11	0.1279	0.3194
13	7	0.4208	0.8799	7	0.1111	0.0151
14	5	0.3779	0.5179	5	0.0775	0.0807
15	5	0.4201	0.6586	7	0.1033	0.2656
16	5	0.4052	0.5568	5	0.3134	0.3727
17	5	0.6587	0.3128	5	0.2803	0.1421
18	5	0.6269	0.4792	5	0.0992	0.1796
19	5	0.2801	0.5103	8	0.1201	0.1013
20	6	0.4136	0.5071	5	0.0255	0.2573
21	5	0.6408	0.3670	9	0.1422	0.0052
22	5	0.3890	0.5743	5	0.3510	0.4110
23	5	0.6245	0.4559	6	0.1006	0.0303
24	5	0.5942	0.4939	7	0.0676	0.0754
25	5	0.4384	0.4662	5	0.1239	0.0052
26	5	0.4184	0.4533	6	0.3116	0.0455
27	7	0.5060	0.5056	5	0.0111	0.0003
28	5	0.4105	0.6626	5	0.0197	0.0169
29	5	0.3373	0.3752	6	0.1104	0.0000
30	7	0.6149	0.2975	5	0.0427	0.0432
Mean	**5.8000**	**0.5002**	**0.5338**	**6.3000**	**0.1480**	**0.1346**
SD	**1.2149**	**0.1178**	**0.1464**	**1.6006**	**0.1100**	**0.1247**

Table 4. ANN (n = 30) analysis of TBARS and GSH levels in the gills of oysters exposed to Cu, Zn and/or Cd.

	Lipid Peroxidation (TBARS)			Glutathione (GSH)		
Model	**#Nodes**	**Model R2**	**CV R2**	**#Nodes**	**Model R2**	**CV R2**
1	5	0.2538	0.0007	9	0.0797	0.0154
2	7	0.2423	0.1488	7	0.0179	0.0647
3	7	0.2578	0.4011	9	0.0635	0.0173
4	6	0.2405	0.1909	5	0.0029	0.0504
5	5	0.1802	0.3001	7	0.0314	0.0003
6	7	0.2687	0.4040	7	0.0726	0.0044
7	8	0.3386	0.2644	8	0.0843	0.0459
8	8	0.4818	0.2464	5	0.0471	0.0413
9	7	0.1684	0.0625	10	0.0697	0.0393
10	11	0.4871	0.2322	9	0.2961	0.0250
11	5	0.4528	0.2011	7	0.0223	0.1310
12	6	0.2826	0.4182	7	0.0674	0.0007
13	6	0.4153	0.4901	6	0.0178	0.1964
14	5	0.5444	0.0489	5	0.0526	0.0022
15	7	0.4401	0.1768	5	0.0498	0.1191
16	8	0.3297	0.2637	11	0.0588	0.0771
17	5	0.4234	0.4465	6	0.0650	0.1535
18	7	0.5074	0.1323	6	0.0344	0.0139
19	9	0.3102	0.1496	7	0.1644	0.0249
20	5	0.3989	0.4732	5	0.0346	0.0899
21	8	0.2456	0.3080	7	0.0346	0.0029
22	5	0.3934	0.5798	5	0.0758	0.0025
23	5	0.5077	0.0112	7	0.0554	0.0097
24	5	0.1863	0.2495	5	0.0793	0.0159
25	5	0.3005	0.0058	8	0.0431	0.0394
26	7	0.2522	0.1038	10	0.0694	0.0328
27	9	0.2899	0.3309	11	0.0732	0.0266
28	5	0.2295	0.2209	9	0.1984	0.0519
29	5	0.4402	0.5114	7	0.1516	0.0122
30	5	0.5173	0.0320	8	0.0652	0.1652
Mean	**6.4333**	**0.3462**	**0.2468**	**7.2667**	**0.0726**	**0.0491**
SD	**1.5906**	**0.1139**	**0.1641**	**1.8370**	**0.0597**	**0.0536**

Figure 1

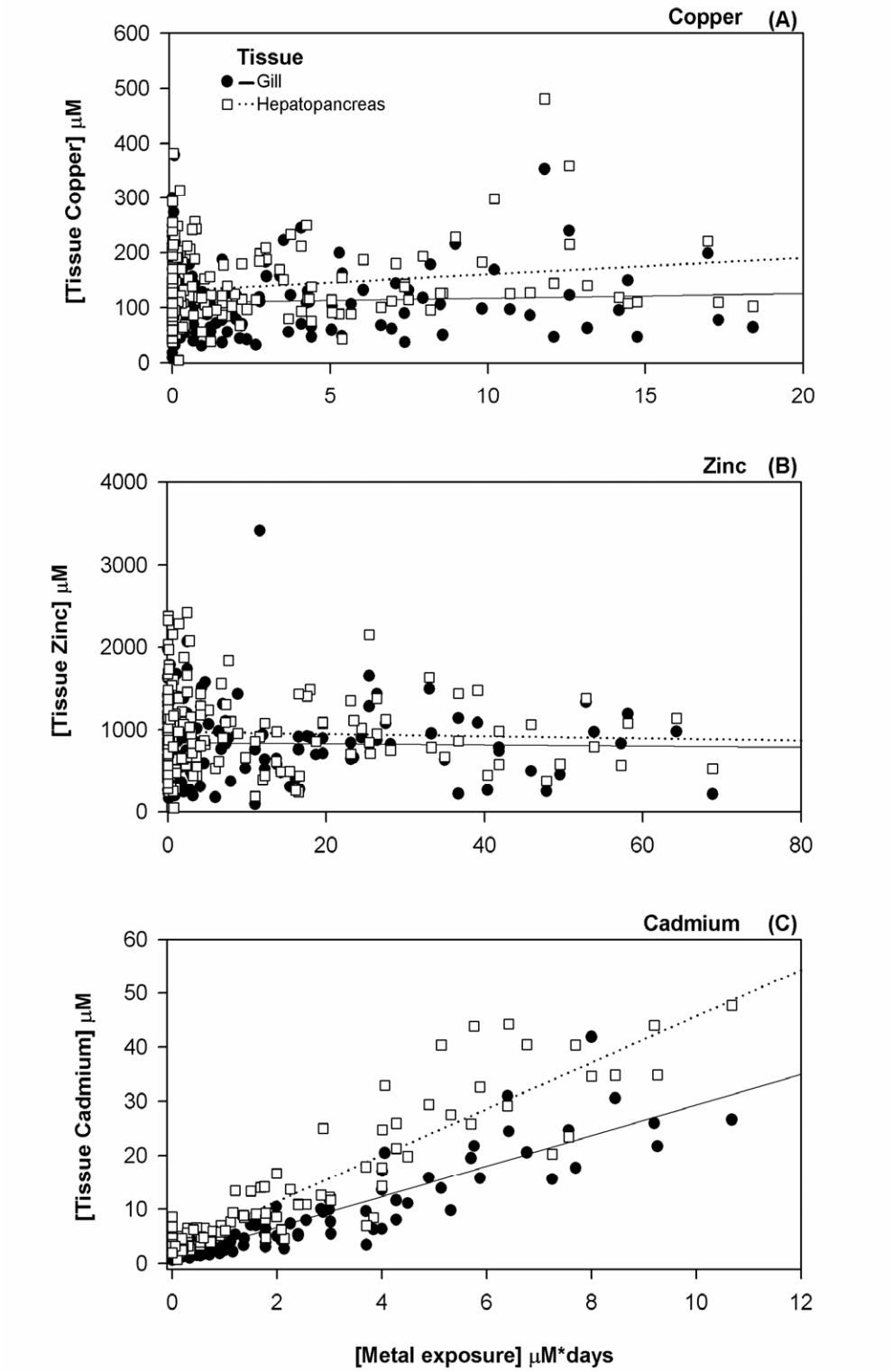

Figure 2

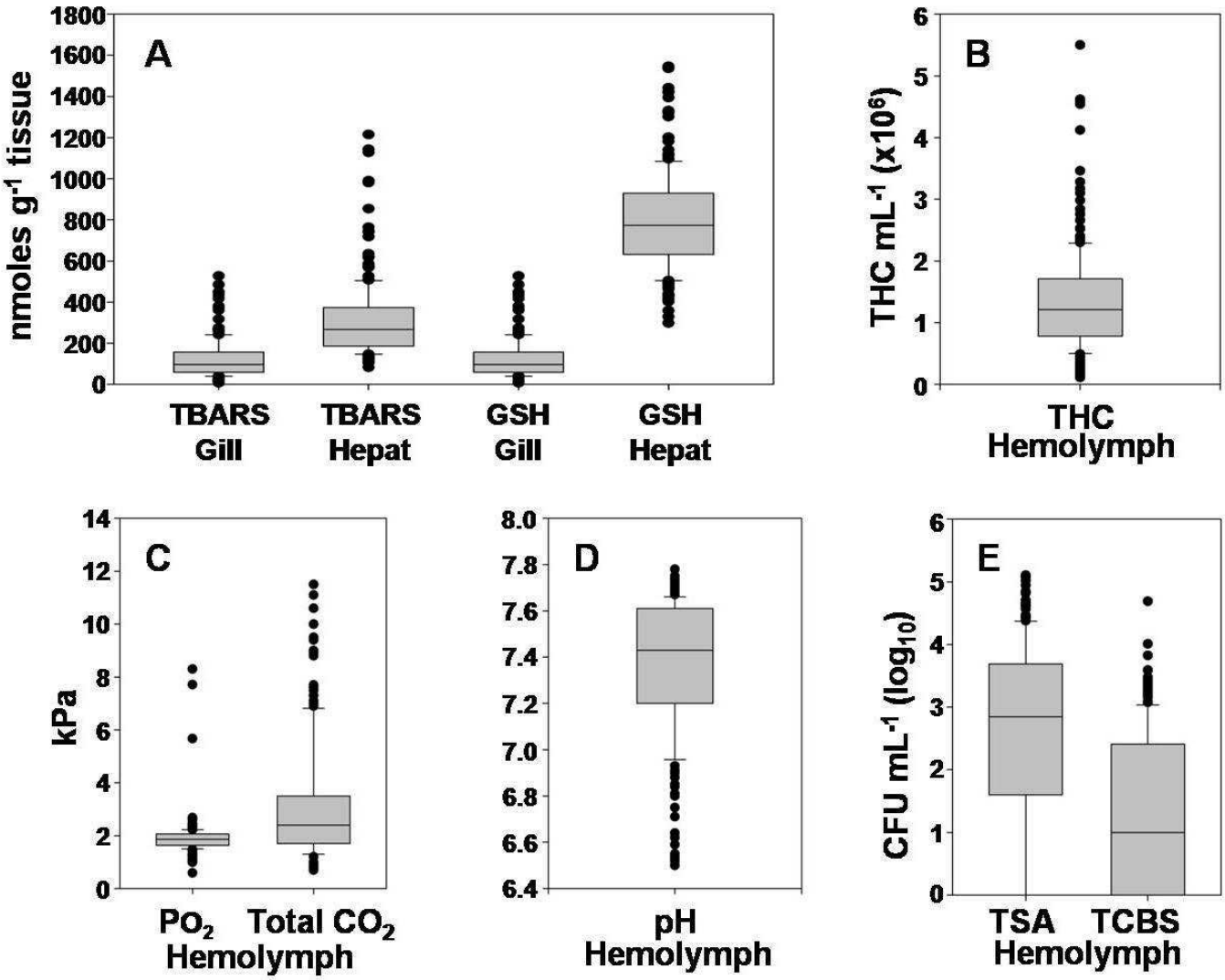

Figure 3

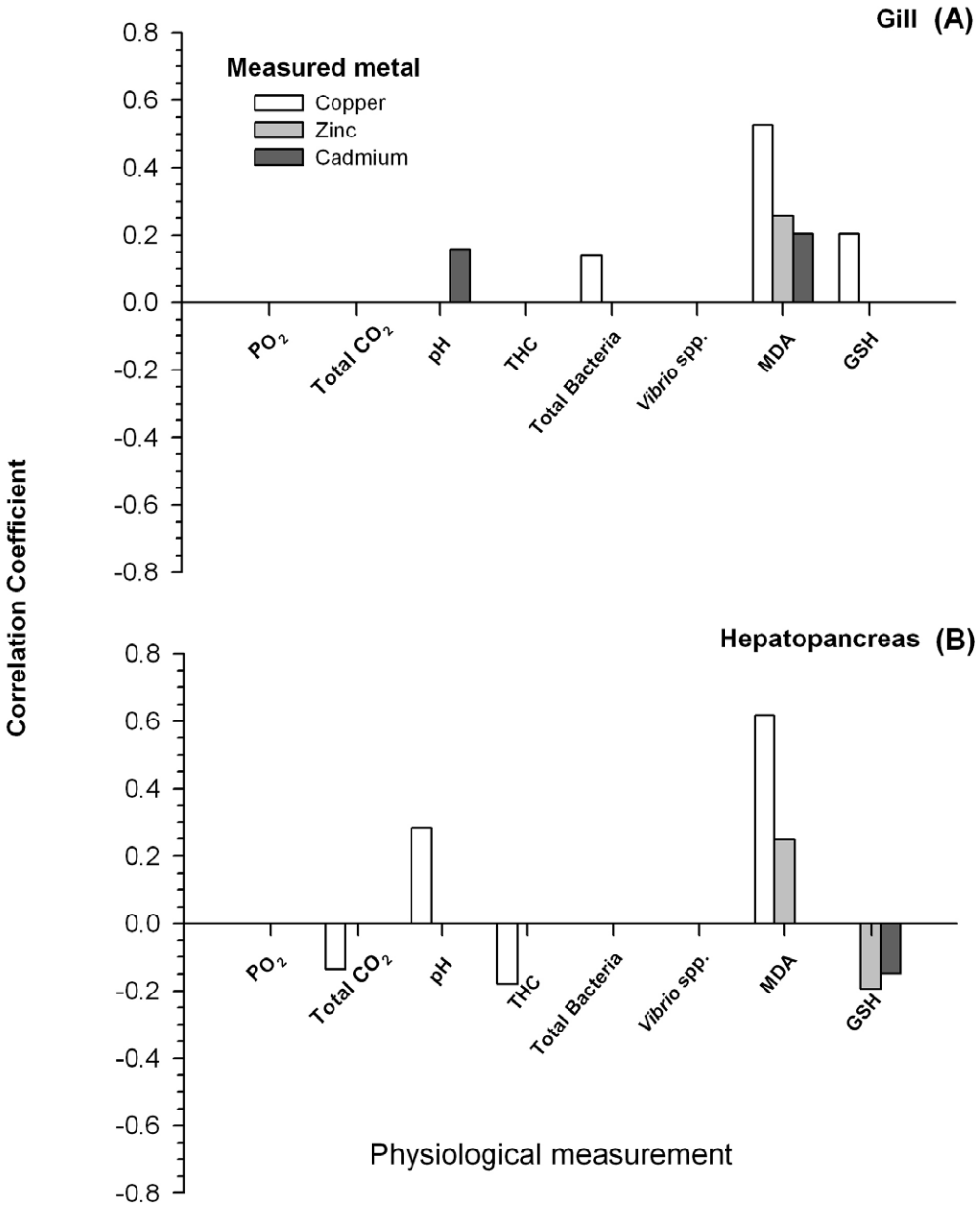

Figure 4

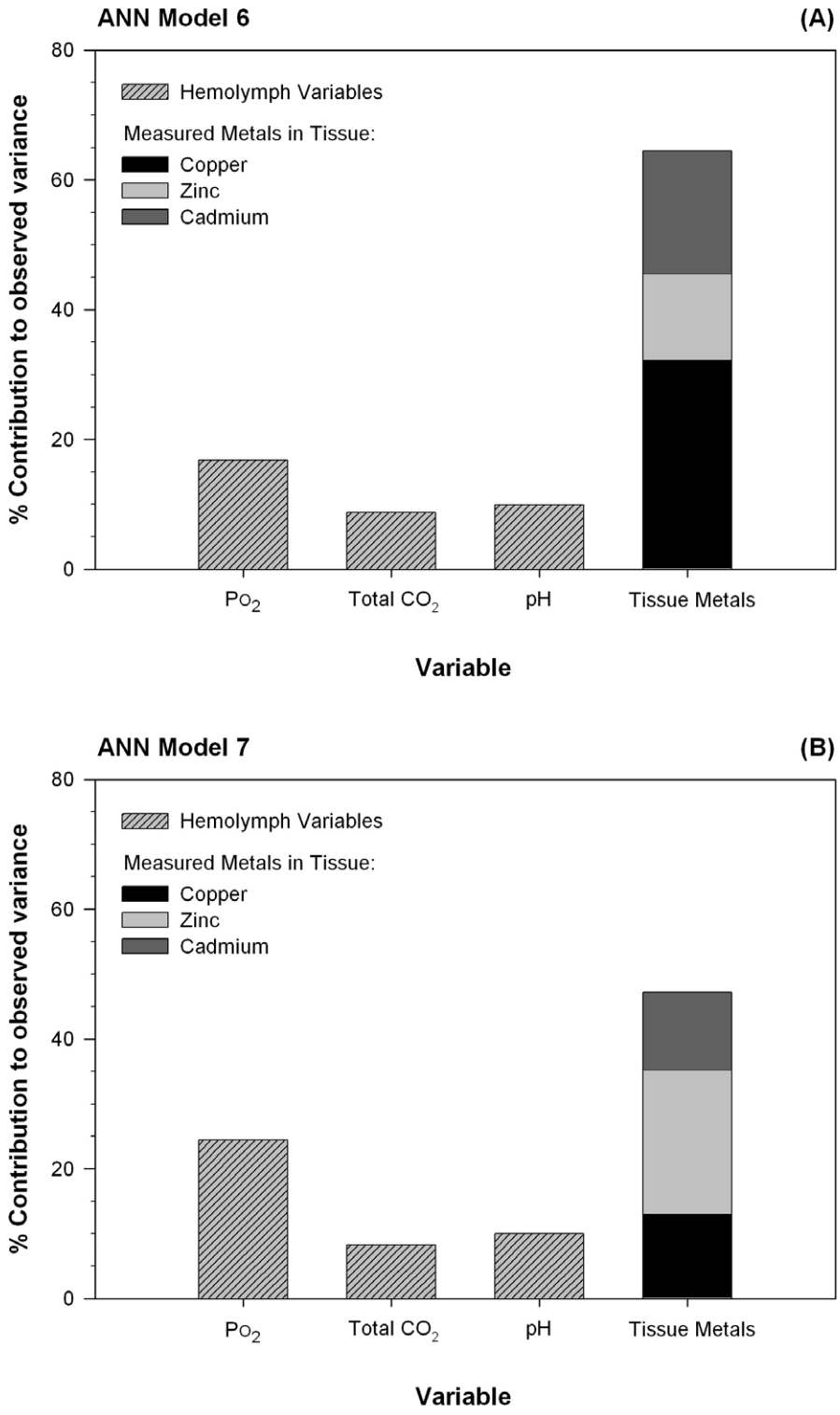

Figure 5

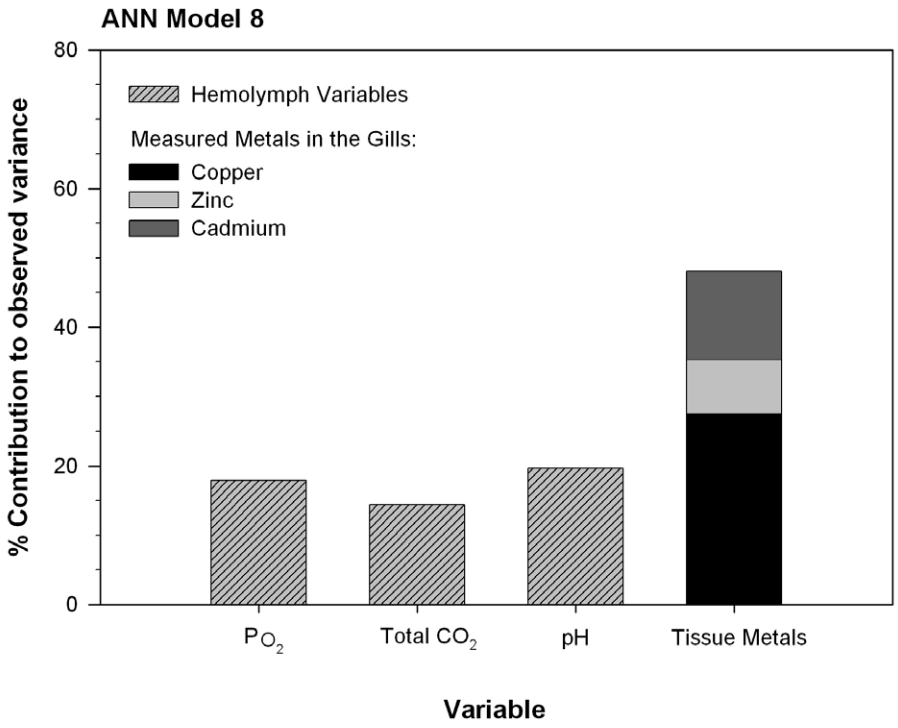

Figure 6